

UC Riverside

UC Riverside Previously Published Works

Title

Tris(1,3-dichloro-2-propyl) Phosphate Exposure During the Early-Blastula Stage Alters the Normal Trajectory of Zebrafish Embryogenesis

Permalink

<https://escholarship.org/uc/item/7110t147>

Journal

Environmental Science and Technology, 52(18)

ISSN

0013-936X

Authors

Dasgupta, Subham
Cheng, Vanessa
Vliet, Sara MF
[et al.](#)

Publication Date

2018-09-18

DOI

10.1021/acs.est.8b03730

Peer reviewed



HHS Public Access

Author manuscript

Environ Sci Technol. Author manuscript; available in PMC 2019 September 18.

Published in final edited form as:

Environ Sci Technol. 2018 September 18; 52(18): 10820–10828. doi:10.1021/acs.est.8b03730.

Tris(1,3-dichloro-2-propyl) phosphate Exposure During Early-Blastula Alters the Normal Trajectory of Zebrafish Embryogenesis

Subham Dasgupta[†], Vanessa Cheng^{†,‡}, Sara M. F. Vliet^{†,‡}, Constance A. Mitchell^{†,‡}, and David C. Volz^{†,*}

[†]Department of Environmental Sciences, University of California, Riverside, California 92521, United States

[‡]Environmental Toxicology Graduate Program, University of California, Riverside, California 92521, United States

Abstract

Tris(1,3-dichloro-2-propyl) phosphate (TDCIPP) is an organophosphate flame retardant used around the world. Within zebrafish, we previously showed that initiation of TDCIPP exposure during cleavage (0.75 h post-fertilization, hpf) results in epiboly disruption at 6 hpf, leading to dorsalized embryos by 24 hpf – a phenotype that mimics the effects of dorsomorphin (DMP), a bone morphogenetic protein (BMP) antagonist that dorsalizes embryos in the absence of epiboly defects. The objective of this study was to 1) investigate the role of BMP signaling in TDCIPP-induced toxicity during early embryogenesis; 2) identify other pathways and processes targeted by TDCIPP; and 3) characterize downstream impacts of early developmental defects. Using zebrafish as a model, we first identified a sensitive window for TDCIPP induced effects following exposure initiation at 0.75 hpf. We then investigated the effects of TDCIPP on the transcriptome during the first 24 h of development using mRNA and amplicon sequencing. Finally, we relied on whole mount immunohistochemistry, dye based labeling, and morphological assessments to study abnormalities later in embryonic development. Overall, our data suggest that initiation of TDCIPP exposure during early blastula alters the normal trajectory of early embryogenesis by inducing

*Phone: (951) 827-4450; Fax: (951) 827 3993; david.volz@ucr.edu.

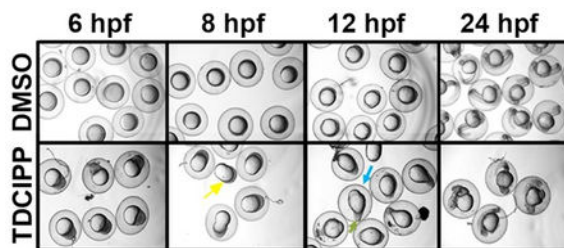
Publisher's Disclaimer: “Just Accepted” manuscripts have been peer-reviewed and accepted for publication. They are posted online prior to technical editing, formatting for publication and author proofing. The American Chemical Society provides “Just Accepted” as a service to the research community to expedite the dissemination of scientific material as soon as possible after acceptance. “Just Accepted” manuscripts appear in full in PDF format accompanied by an HTML abstract. “Just Accepted” manuscripts have been fully peer reviewed, but should not be considered the official version of record. They are citable by the Digital Object Identifier (DOI®). “Just Accepted” is an optional service offered to authors. Therefore, the “Just Accepted” Web site may not include all articles that will be published in the journal. After a manuscript is technically edited and formatted, it will be removed from the “Just Accepted” Web site and published as an ASAP article. Note that technical editing may introduce minor changes to the manuscript text and/or graphics which could affect content, and all legal disclaimers and ethical guidelines that apply to the journal pertain. ACS cannot be held responsible for errors or consequences arising from the use of information contained in these “Just Accepted” manuscripts.

Supporting Information

A Microsoft Excel spreadsheet containing 1) processed and analyzed mRNA sequencing data; 2) raw data for normalized read counts of maternal and zygotic transcripts used in Figure 2; 3) raw data from amplicon-sequencing (Table S1); 4) raw data from oxygen consumption assays (Figure S7); and 5) experimental design details as well as raw data supporting Figures 1 and S1 are provided within Supplemental File 1. Supplemental File 2 contains Table S1 and Figures S1–S10. This information is available free of charge via the Internet at <http://pubs.acs.org>. The authors declare no competing financial interest.

gastrulation defects and aberrant germ layer formation, leading to abnormal tissue and organ development within the embryo.

TOC/Abstract Art



Introduction

Early vertebrate embryogenesis is regulated by dynamic processes that have the potential to be sensitive to environmental chemical exposure. Immediately after fertilization, the single-celled zygote undergoes cleavage to form a multicellular blastula and, during gastrulation, germ layers (ectoderm, mesoderm, and endoderm) are formed by rapid cellular proliferation; each of these germ layers have different cell fates that ultimately give rise to different tissues and organs within the developing embryo. Chemical exposures during early development may target blastula and/or gastrula, resulting in abnormal cell migration, germ layer formation, and dorsoventral patterning. For example, *in utero* exposure to alcohol in mammals results in craniofacial, neural, and cardiac deformities.¹ In mammals, aberrant embryogenesis during the pre implantation period can also lead to failed uterine implantation and premature abortion of the embryo.² In model organisms such as zebrafish and *Xenopus*, germ layer formation is preceded by epiboly – a process primarily dependent on microtubule dynamics and activity of cell adhesion molecules.^{3, 4} Epiboly is known to be sensitive to chemicals like perfluorooctanesulfonic acid and ethanol, leading to the formation of embryos with structural defects.^{5, 6}

Disruption of the normal trajectory of embryogenesis is usually caused by targeted effects of chemicals on a network of transcriptomic, biochemical, and epigenetic pathways that regulate development. For example, epidemiological studies have shown that human exposure to chemicals like persistent organic pollutants, metals, and cigarette smoke are associated with alterations in epigenetic processes that modulate the maternal-to-zygotic transition (MZT), leading to later life consequences like behavioral abnormalities and cancer.⁷ Similarly, certain chemicals may target gastrulation by influencing development specific signaling pathways, resulting in disruption of germ layer formation, organogenesis, and dorsoventral patterning.⁸

Organophosphate flame retardants (OPFRs) are commonly used around the world in consumer products such as furniture, electronics, automobiles, and children's products (e.g., car seats, baby clothing, and juvenile furniture). Due to the potential to leach from end use products into indoor dust, concerns remain about the effects of OPFRs in human populations following inhalation, ingestion, and/or dermal exposure.^{9, 10} In particular, the first eight

weeks of human development (the embryonic period) may be susceptible to the potential effects of OPFR exposure, as this period of development encompasses many coordinated, dynamic processes that are critical for successful implantation and tissue differentiation. Tris(1,3-dichloro-2-propyl) phosphate (TDCIPP) is a high production volume OPFR that is used throughout the United States. Elevated concentrations of TDCIPP have been detected in dust samples collected within the built environment.^{9, 11} As a result, TDCIPP and bis(1,3-dichloro 2 propyl) phosphate (BDCIPP, the primary metabolite of TDCIPP) have also been detected from urine and dermal samples of toddlers¹², pregnant mothers¹³, placental samples¹⁴ and, in a recent study, 92% of a representative sampling of the United States population.¹⁵ Moreover, recent studies have linked prenatal TDCIPP exposures in pregnant women to decreased gestational length⁹ and fertilization rates in couples undergoing *in vitro* fertilization.¹⁶

Using zebrafish as a model, several recent studies have demonstrated that TDCIPP disrupts early developmental processes. TDCIPP exposures starting at cleavage (within the first 2 hours post fertilization, hpf) result in epiboly delay or arrest during gastrulation (4–6 hpf)^{17,19}, and surviving embryos exhibit a range of malformations by 96 hpf.²⁰ In addition, TDCIPP-induced epiboly results in dorsalized phenotypes by 24 hpf, and TDCIPP-induced dorsalization (but not epiboly defects) phenocopy dorsomorphin (a bone morphogenetic protein, or BMP, antagonist), suggesting that BMP signaling may be disrupted by TDCIPP following epiboly.¹⁷ Therefore, the first objective of this study was to identify a sensitive window of TDCIPP-induced toxicity during blastula/gastrula and characterize phenotypic changes following epiboly. Using a combination of mRNA-sequencing as well as pharmacologic and immunohistochemical strategies, our second objective was to investigate the impact of TDCIPP on BMP signaling and identify other potential pathway targets of TDCIPP during the first 24 h of development. Within this objective, we also assessed whether TDCIPP exposure induced delays in zygotic genome activation within the first 3–4 h of development. Based on our mRNA-sequencing data, our final objective was to determine whether TDCIPP-induced changes in the transcriptome were associated with downstream phenotypic effects at later stages of embryonic development.

Methods

Animals

Adult wildtype (5D) zebrafish were maintained and bred on a recirculating system using previously described procedures.²¹ Adult breeders were handled and treated in accordance with an Institutional Animal Care and Use Committee (IACUC)-approved animal use protocol (#20150035) at the University of California, Riverside.

Chemicals

TDCIPP (99% purity) was purchased from ChemService; dorsomorphin (DMP) (99.7% purity), 4'-hydroxychalcone (4'H) (purity unavailable), and butafenacil (99.3% purity) were purchased from Sigma-Aldrich. For all three chemicals, stock solutions were prepared in high performance liquid chromatography (HPLC)-grade dimethyl sulfoxide (DMSO) and stored within 2-mL amber glass vials with polytetrafluoroethylene lined caps. Working

solutions were prepared in embryo media (5 mM NaCl, 0.17 mM KCl, 0.33 mM CaCl₂, 0.33 mM MgSO₄, pH 7) immediately prior to each experiment.

Embryo Exposures and Phenotyping

All embryos were staged according to previously described methods.²² Viable 5D embryos at the 2-cell stage (0.75 hpf) were exposed to 10 mL of vehicle (0.1% DMSO), TDCIPP (0.78, 1.56, or 3.12 μM), DMP (0.312 or 0.625 μM) and/or 4'H (5 μM) in clean 60-mm glass petri dishes. For all assessments, nominal concentrations of TDCIPP (1.56 μM and 3.12 μM) and DMP (0.312 μM) were based on our prior studies relying on epiboly defects and dorsalization as readouts¹⁷; a single nominal concentration of 5 μM 4'H was also identified as the maximum tolerated concentration based on initial range-finding exposures that relied on survival and ventralization as endpoints. All exposures were conducted under static conditions at 28°C within a temperature-controlled incubator under a 14-h:10-h light:dark cycle. Results from previous studies in our laboratory have shown that, following initiation of exposure at 0.75 hpf, there is significant embryonic uptake of TDCIPP by 2 hpf in the absence of BDCIPP formation.^{20, 23} At exposure termination, petri dishes were removed from the incubator, coagulated embryos discarded, and live embryos were imaged under transmitted light using a Leica MZ10 F stereomicroscope (Leica Microsystems, Inc.) equipped with a DMC2900 camera. For epiboly and dorsalization assessments, one-way or two-way analysis of variance (ANOVA) models were performed in R (www.r-project.org) based on the percentage of normal embryos within each group; pair-wise Tukey-based multiple comparisons were performed to identify significant treatment related effects relative to vehicle controls.

mRNA-Sequencing

To assess the effects of TDCIPP on the transcriptome, embryos were exposed to vehicle (0.1% DMSO), 1.56 μM TDCIPP, 3.12 μM TDCIPP, or 0.625 μM DMP (20 embryos per replicate; 3 replicates per treatment by stage) at 0.75 hpf and snap frozen in liquid nitrogen at 4, 6, 8, 10, 12 and 24 hpf; in addition, vehicle-and TDCIPP-treated embryos were sampled at 3 and 5 hpf. All samples (90 total) were then stored at -80°C until total RNA extraction. All embryos were homogenized in 2-ml cryovials using a PowerGen Homogenizer (Thermo Fisher Scientific) and, following homogenization, an SV Total RNA Isolation System (Promega) was used to extract total RNA from each replicate sample per manufacturer's instructions. RNA quantity and quality were confirmed using a Qubit 3.0 Fluorometer and 2100 Bioanalyzer system, respectively. Based on sample specific Bioanalyzer traces, the RNA Integrity Number (RIN) was >8 for all RNA samples used for library preparations.

Libraries were prepared using a Lexogen Quantseq 3' mRNA Seq Library Prep Kit FWD, and mRNA-sequencing and bioinformatics were performed as previously described²⁴; libraries derived from all treatments within each time point were sequenced in a single flow cell, resulting in a total of eight flow cells. Raw Illumina (fastq.gz) sequencing files (90 files) are available via NCBI's BioProject database under BioProject ID PRJNA475635, and a summary of sequencing run metrics are provided in Supplemental File 1 (>90% of reads were Q30 across all runs). A false discovery rate (FDR) *p* adjusted value < 0.05 was used

as the threshold for identifying significant differences in transcript abundance. Significantly affected transcripts were imported into DAVID Bioinformatics Resources 6.8 for Gene Ontology (GO) enrichment analysis against zebrafish genome assembly GRCz10 as previously described.¹⁷ For identifying potential impacts on zygotic genome activation, all libraries derived from vehicle (0.1% DMSO), 1.56 μ M TDCIPP, and 3.12 μ M TDCIPP treatments were normalized in Bluebee's DESeq2 application (Lexogen Quantseq DE 1.2), and the sum of normalized counts of maternal or zygotic transcripts obtained from Harvey et al. 2013²⁵ were calculated (Supplemental File 1).

Amplicon-Sequencing

Based on differentially expressed genes derived from mRNA-sequencing and a subset of other targets specific to related pathways, we selected 30 transcripts total for amplicon sequencing (Supplemental File 1). Primer sets were designed to amplify ~300–400 bp of each target and synthesized by Integrated DNA Technologies. Total RNA extracted from embryos exposed to vehicle (0.1% DMSO) and 3.12 μ M TDCIPP from 0.75 hpf to 3, 6 or 12 hpf (50 embryos per replicate; 3 replicates per treatment by stage) were reverse transcribed using a GoScript Reverse Transcription System (Promega) and targets were amplified using a 25 μ L reaction mixture containing ZymoTaq (Zymo Research), 20 ng of cDNA, and the following PCR conditions: 10 min at 95°C followed by 38 cycles of 95°C for 30s, 50°C for 30s, 72°C for 30s, with a final extension of 72°C for 7 min. PCR products were then purified using a QIAquick 96 PCR Purification Kit (Qiagen), and amplicon quality was confirmed using a 2100 Bioanalyzer system and DNA 1000 kits from Agilent. Following confirmation of amplicon concentrations using a Qubit 3.0 Fluorometer, amplicons were pooled by treatment replicate and diluted to a concentration of 0.2 ng/ μ L. Libraries were then prepared using Illumina's Nextera XT DNA Library Prep kit and indexed by treatment replicate. Similar to previously described procedures¹⁸, all libraries were then pooled, diluted to a concentration of 1.3 pM (with 25% PhiX control), and paired-end (2X150) sequenced on our Illumina MiniSeq Sequencing System using a single 300-cycle Mid Output Reagent Kit. All sequencing data were uploaded to Illumina's BaseSpace in real-time for downstream analysis of quality control. Raw Illumina (fastq.gz) sequencing files (36 files) are available via NCBI's BioProject database under BioProject ID PRJNA475635, and a summary of sequencing run metrics are provided in Supplemental File 1 (90.3% of reads were Q30). All 36 raw and indexed Illumina (fastq.gz) sequencing files were then imported into the RNA Seq Alignment application within BaseSpace, and alignment was performed using the STAR aligner and zebrafish danRer7 genome assembly. Following alignment of reads, significant differences in transcript abundance were detected using the DESeq2 application within BaseSpace based on a q threshold of 0.05.

Whole-Mount Immunohistochemistry

At exposure termination, embryos were dechorionated using 100 mg/L pronase, fixed overnight in 4% paraformaldehyde (PFA) in 1X phosphate buffered saline (PBS), and then stored in PBS at 4°C. Fixed embryos were then incubated with anti phospho SMAD 1/5/9 IgG (1:100 dilution, Cell Signaling), anti Tbx16 IgG₂ (anti-VegT, 1:10, Zebrafish International Resource Center), or anti-zn-8 IgG₁ (1:20, Developmental Studies Hybridoma Bank, University of Iowa) following previously described protocols.²⁶ Embryos were

incubated with IgG-, IgG₂-, or IgG₁-specific Alexa Fluor conjugated secondary antibodies (Sigma) and imaged at 8X magnification using a Leica MZ10 F stereomicroscope equipped with a GFP filter and DMC2900 camera.

Hemoglobin Staining

To measure hemoglobin levels within developing embryos, embryos were euthanized with MS-222 at 72 hpf and stained with *o*-dianisidine using previously described protocols.²⁷ All embryos were oriented in dorsal recumbency and imaged against a black background under transmitted light at 4X magnification using a Leica MZ10 F stereomicroscope equipped with a DMC2900 camera. Treatment-specific differences were identified using an ANOVA followed by Tukey's post hoc test ($p < 0.05$) within R.

Pericardial Area and Cardiac Assessments

After exposure to TDCIPP from 0.75–24 hpf, embryos were transferred to clean embryo media until 72 hpf, and then anesthetized and imaged at 3.2X (for pericardial area) and 8X (for cardiac morphology) magnification using a Leica MZ10 F stereomicroscope equipped with a DMC2900 camera. Pericardial area (a biomarker for cardiac looping defects) was quantified within Image J, and treatment specific differences were identified using a one way ANOVA model followed by Tukey based multiple comparison procedures within R.

Ocular Area and Pigmentation Assessments

After exposure to TDCIPP from 0.75–24 hpf, embryos were transferred to clean embryo media until 48 hpf, and then dechorionated, anesthetized, and imaged at 3.2X (for body length) and 8X (for eye measurements) magnification using a Leica MZ10 F stereomicroscope equipped with a DMC2900 camera. Eye area and pigmentation were quantified within Adobe Photoshop; for pigmentation, the darkest shade of black pigment was replaced with red using the "Replace Color" tool, and the area of the red hue within the eye was quantified similar to *o*-dianisidine measurements. Treatment specific differences were identified using a one-way ANOVA model followed by Tukey-based multiple comparison procedures within R.

Results

Sensitive Window of Exposure for TDCIPP-Induced Deformities

Based on TDCIPP-induced epiboly and dorsalization phenotypes observed within our previous study¹⁷, we sought to identify the most sensitive window for these effects by initiating exposures at different time points starting at 0.75 hpf. Relative to initiation of exposure at 2 hpf, we found that initiation of exposure at 3 hpf resulted in a statistically significant increase in percentage of normal embryos at both 6 hpf (Figure 1A) and 24 hpf (Figure S1A), indicating that 2–3 hpf is a highly sensitive window for TDCIPP-induced developmental toxicity during early embryogenesis.

Effect of Pre-treatment with 4'-H on TDCIPP-Induced Deformities

To investigate whether TDCIPP-induced abnormalities were blocked by a BMP agonist (4'H), we pre-treated embryos to 5 μ M 4'H from 0.75–2 hpf, followed by exposure to 3.12 μ M TDCIPP or 0.312 μ M DMP from 2–6 hpf. Interestingly, pre-treatment with 4'H partially blocked the severity of epiboly and dorsalization phenotypes, resulting in a statistically significant increase in proportion of normal embryos at 6 hpf (Figure 1B) as well as a similar (albeit non-significant) increase in proportion of normal embryos at 24 hpf (Figure S1B).

Effect of TDCIPP on Zygotic Genome Activation

As 2–3 hpf overlaps with the onset of the MZT, we assessed whether TDCIPP has the potential to delay zygotic genome activation. Based on normalized read counts of maternal and zygotic transcripts²⁵, we observed a slight ~1-h delay (relative to vehicle controls) in activation of zygotic transcripts in TDCIPP-exposed embryos at 3 hpf in the absence of effects on maternal transcript abundance; however, this effect was not statistically significant due to variation in zygotic transcript abundance at 3 hpf within the vehicle controls (Figure 2). Importantly, there were also no significant differences in transcript abundance for three highly translated, maternally loaded transcription factors (*nanog*, *pou5f3*, and *sox19b*) that are known to regulate MZT (Table S1).

Overlap of TDCIPP- and DMP-Affected Pathways

Volcano plots in Figure S2 represent overall results from mRNA-sequencing, Supplemental File 1 provides data for significantly affected transcripts from all treatments, and Table S1 shows fold changes and functions of a subset of transcripts. While 1.56 μ M TDCIPP induced minimal effects on the transcriptome, changes in transcript abundance following exposure to 3.12 μ M TDCIPP and 0.625 μ M DMP were dependent on the stage of embryonic development. Maximal responses for all treatments were seen at 24 hpf, with concentration-dependent responses for 19 transcripts between both TDCIPP treatments (Figure S3). At 3 and 6 hpf, transcript levels of gastrulation-regulating genes (*cyt1* and *apoc1*) were decreased by TDCIPP based on mRNA- and amplicon-sequencing (Table S1). Surprisingly, despite phenotypic similarities at 24 hpf¹⁷, there was minimal overlap between transcripts affected by TDCIPP and DMP during the first 12 h of development (Figure S4). Importantly, mRNA levels of BMP pathway relevant genes that were differentially affected by DMP (*bmp7a*, *vox*, and *bambia*) were not impacted by TDCIPP (Figure 3A); the only exception was sizzled (*szl*), which was consistently decreased following exposure to both TDCIPP and DMP (Figure 3B).

The absence of effects on BMP signaling was also confirmed by immunostaining. Contrary to DMP, a ventral-to-dorsal gradient of BMP signaling (using anti-phospho-SMAD 1/5/9) was not affected within embryos exposed from TDCIPP from 0.75 to 8 hpf (Figure 3C). As the number of significantly affected transcripts during each exposure window prior to 12 hpf was low, we combined data from 10 and 12 hpf to assess pathway-level effects during the onset of somitogenesis and found that pathways involved in mesoderm development, somitogenesis, and brain/retinal development were significantly impacted (Figure S5A). Using data derived from 0.75–24 hpf exposures, GO analysis revealed significant effects on

numerous pathways including oxygen transport, microtubules, hematopoiesis, brain development, mitochondrial function, and oxidative phosphorylation (Figure S5B).

TDCIPP-Induced Effects on Mesoderm Development and Differentiation

During early somitogenesis, TDCIPP decreased transcripts (*msgn1*, *tbx6*, *tbx6l*, and *tbx16*) that directly regulate mesoderm development and differentiation (Figure 4A; Table S1). Transcript levels of *sp5l* – a Wnt-regulated gene that also regulates mesoderm differentiation – was increased at 6 hpf (Table S1). Consistent with mRNA-sequencing results, amplicon-sequencing (Table S1) showed a >4-fold and ~1.5-fold decrease in *tbx6* transcripts at 3 and 12 hpf, respectively; transcript levels of *ta* – a gene also associated with mesoderm differentiation – was decreased by ~1.9-fold. Indeed, immunostaining with anti-Tbx16 (a marker of paraxial mesoderm) also revealed aberrant localization of mesodermal cells in TDCIPP-treated embryos by 12 hpf. However, although a more extensive phenotypic assessment revealed that TDCIPP and DMP-treated embryos appeared morphologically similar starting at ~10 hpf (post-gastrulation) (Figure S6), Tbx16 localization within DMP-treated embryos at 12 hpf was not affected (Figure 4B). Observation of embryos under a higher magnification revealed that, despite apparent phenotypic similarities, TDCIPP-treated embryos lacked the presence of a well defined notochord and somites, while DMP-treated embryos retained these structures – although the somites were more radially extended compared to vehicle controls (Figure 4C).

TDCIPP-Induced Effects on Hemoglobin Levels and Oxygen Consumption

As red blood cells are derived from the mesoderm, we also determined whether TDCIPP impacted hemoglobin levels and oxygen consumption following somitogenesis. Additional details about oxygen consumption assays are provided within the Figure S7 legend. Interestingly, TDCIPP exposure resulted in a significant decrease in the abundance of *gata1a* (an erythroid transcription factor) by 12 hpf and other hemoglobin specific transcripts by 24 hpf (Table S1). Moreover, there was a significant concentration dependent decrease in hemoglobin levels following exposure from 0.75–24 hpf (Figure 5A) – an effect that occurred in the absence of alterations on embryonic oxygen consumption (Figure S7; Supplemental File 1). However, the impacts on TDCIPP on hemoglobin levels were absent when exposures were initiated at 10 hpf (post gastrulation) (Figure S8A).

TDCIPP-Induced Effects on Cardiac Development

As cardiomyocytes are also derived from the mesoderm, we assessed the impacts of TDCIPP on cardiac development. At 24 hpf, TDCIPP exposures decreased levels of transcripts specific to cardiac development (Table S1). In addition, exposure to 3.12 μ M TDCIPP from 0.75–24 hpf resulted in a concentration dependent increase in pericardial area by 72 hpf (Figure 5B), with ~40% of embryos exhibiting cardiac looping defects (Figure 5B inset). Similar to effects on hemoglobin levels, this effect was absent when exposures were initiated at 10 hpf (post gastrulation) (Figure S8B).

TDCIPP-Induced Effects on Eye and Brain Development

Although GO analysis indicated that TDCIPP impacted eye development, the majority of eye development related transcripts were increased; *smarca5* – a gene associated with retinal development – was the only transcript decreased at 24 hpf (Table S1). To investigate whether these effects were associated with eye defects later in development, we quantified ocular area and pigmentation at 48 hpf and observed a concentration dependent decrease in ocular area as well as pigmentation within TDCIPP treated embryos (Figures 5C and 5D). Embryos immunostained with zn-8 antibody also revealed a lack of neuronal growth within the developing eye at 48 hpf (Figure S9). Although TDCIPP exposures decreased transcripts associated with brain development (Table S1), no visible effects on brain morphology were observed in zn-8-labeled embryos by 48 hpf (Figure S10).

Discussion

Using zebrafish as a model, the objective of this study was to investigate the effects of TDCIPP on the trajectory of early embryonic development. We first showed that TDCIPP-induced effects on epiboly and dorsoventral patterning were primarily restricted to exposures initiated during cleavage (by ~2 hpf), and that there was a strong decrease in abnormalities if exposures were initiated at mid blastula (3 hpf). We also showed that TDCIPP-treated embryos phenocopied DMP-treated embryos starting at ~10 hpf (post gastrulation), where TDCIPP-and DMP-exposed embryos developed an ovoid shape and exterior tissue masses that ultimately led to dorsalization. These findings are consistent with our previous study²⁰ and establishes cleavage (0.75–2 hpf) and early blastula (2–3 hpf) as sensitive windows for TDCIPP-induced effects on both epiboly and dorsoventral patterning.

Early-blastula (2–3 hpf) is also marked by initiation of zygotic genome activation (ZGA).²⁸ Using normalized read counts, our data suggests that TDCIPP may induce a slight delay in ZGA, albeit in the absence of impacts on key maternally loaded transcriptional factors that regulate ZGA (*nanog*, *pou5f3*, and *sox19b*).²⁹ Since epiboly progression is dependent on zygotic transcription^{5, 30}, the ZGA delay may be responsible for subsequent delays in epiboly. Epiboly defects may also have resulted from TDCIPP induced decreases in transcripts of gastrulation regulating genes (*cyt1* and *apoc1*), as epiboly is delayed within embryos deficient in these transcripts.^{31, 32} However, further studies are needed to identify mechanisms that lead to distinct epiboly phenotypes (delay vs. arrest) within an identical TDCIPP treatment group.

As our previous study showed that TDCIPP-exposed embryos phenocopied DMP induced dorsalization by 24 hpf, we hypothesized that TDCIPP inhibits BMP signaling. Indeed, pre-treatment with 4'H (a weak BMP agonist) partially blocked TDCIPP-and DMP-induced dorsalization, where 55% and 40% of embryos pre-treated with DMSO or 4'H, respectively, were dorsalized. However, results from mRNA-sequencing showed that TDCIPP-induced minimal effects on BMP signaling during these stages; in particular, contrary to DMP, TDCIPP did not result in significant impacts on transcripts associated with the BMP signaling pathway. The absence of impacts on BMP signaling was also confirmed by immunostaining embryos with anti p SMAD 1/5/9, which labels SMAD proteins specific to the ventral to dorsal BMP signaling gradient during gastrulation.³³ The BMP gradient

within TDCIPP-treated embryos was similar to vehicle controls, suggesting that BMP signaling is likely not a major target of TDCIPP. However, *szl* – a BMP pathway inhibitor – was significantly decreased in both TDCIPP and DMP treatments. In our prior microarray-based study¹⁷, we observed a similar TDCIPP induced decrease in *szl* at 6 hpf; however, since *szl* morphant embryos did not phenocopy TDCIPP induced epiboly defects and dorsalization, the role of TDCIPP-induced decreases in *szl* remains unclear. Furthermore, as 4'H partially blocked epiboly defects in TDCIPP-treated embryos, our data suggest that 4'H and TDCIPP may share a common target that regulates epiboly and gastrulation movements but is not directly related to the BMP signaling pathway.

Interestingly, GO pathway analysis revealed that TDCIPP directly affected transcripts regulating mesoderm specification. During gastrulation, a feedback loop between Wnt signaling and Ntl maintains the undifferentiated state of mesodermal progenitor cells (MPCs); *msgn1* and *tbx16* overexpression inhibits this Wnt-Ntl loop, resulting in differentiation of MPCs into tail and trunk mesoderm that further differentiate into tail and trunk somites.³⁴ In our experiments, TDCIPP induced a significant increase in *sp51* (a Wnt-regulated gene) at 6 hpf, followed by decreased levels of *msgn1*, *tbx16*, *tbx6*, and *tbx6l* – all of which regulate mesoderm development, specification and differentiation^{35–38} – by early segmentation (10–12 hpf). Decreased abundance of *ta* transcripts observed at 12 hpf may also contribute to mesodermal disruption, as *ta* interacts with *msgn1* to regulate mesoderm differentiation during somitogenesis.³⁴ Immunostaining with anti Tbx16 at 12 hpf further revealed a disruption in localization of mesodermal cells in TDCIPP-treated but not DMP-treated embryos. Collectively, these phenotypic and transcriptomic data indicate that TDCIPP may primarily impact mechanisms that regulate gastrulation and mesoderm development. However, since BMP signaling, in part, regulates mesodermal differentiation³⁹, there may be an indirect effect of TDCIPP on proteins involved in the BMP signaling pathway.

We then focused on investigating impacts of TDCIPP on embryonic structures derived from the mesoderm. We initially characterized the development of somites and notochord – the first structures that are derived from the mesoderm.⁴⁰ Consistent with mesodermal disruption, TDCIPP-treated embryos lacked the presence of well-defined somites or notochord at 12 hpf. These phenotypes are consistent with double-morphants deficient in *tbx16* and *msgn1*, as these genes are essential for differentiation of mesodermal cells.⁴¹ In particular, as somites are derived from the paraxial mesoderm⁴², the absence of somite development was consistent with disrupted mesoderm based on immunostaining with anti Tbx16 – a marker of paraxial mesoderm. In contrast to TDCIPP-treated embryos and consistent with previous studies⁴³, DMP treated embryos contained an intact notochord and somites in the posterior region although, in most cases, these somites did not fully extend into the anterior side and showed a broader radial extension compared to vehicle controls. Consistent with our mRNA-sequencing data, these subtle structural differences between TDCIPP and DMP-treated embryos also highlight the different modes of action for these two compounds.

Downstream in the developmental trajectory, mesodermal tissues differentiate into red blood cells as well as cardiomyocytes.³⁴ Tbx16 also plays an important role in the differentiation

of mesodermal cells into red blood cells.^{38, 44} In our study, when exposures were initiated at 0.75 hpf, TDCIPP-exposed embryos were, similar to an anemia-inducing herbicide (butafenacil)⁴⁵, anemic by 72 hpf in a concentration-dependent manner. These results corroborated TDCIPP-induced disruption of localization of mesodermal cells *in situ*, as well as a decrease in levels of *tbx16* and red blood cell specific genes such as *gata1* (at 12 hpf) and *hbae3*, *hbbe3*, *hbbe1.2* and *hbae1.3* (at 24 hpf). As these genes regulate hemoglobin synthesis and the oxygen carrying capacity of the blood, we investigated oxygen consumption by the embryo following a 0.75–24 hpf exposure to TDCIPP. However, we found no significant effect on oxygen consumption, as early stage embryos obtain oxygen by diffusion through the skin rather than blood driven convective transport.⁴⁶ TDCIPP also impacted cardiac development, where embryos exposed to TDCIPP from 0.75–24 hpf displayed a concentration-dependent increase in pericardial edema, a marker for cardiac defects⁴⁷ by 72 hpf. Similarly, by 24 hpf, TDCIPP exposures decreased the abundance of heart specific transcripts (*bin1b*, *tnni2b.1*, *tnni2a.4*, *lrrc39*, *tnnb*, and *ttn.2*), indicating a dysregulation of cardiac development and function; indeed, embryos deficient in *lrrc39* and *ttn* are known to have defects in cardiac contractility.^{48, 49} Furthermore, GO pathway analysis at this stage also showed effects on cardiac muscle fiber development and tissue morphogenesis. However, severe pericardial edema or anemia was absent when exposures were started post gastrulation (~10 hpf), indicating that these TDCIPP-induced impacts were likely specific to disruption of earlier developmental processes such as gastrulation and mesoderm differentiation.

Based on GO pathway analysis, we also investigated the impacts of TDCIPP exposures on eye and brain development. While we did not observe gross malformations in the brain based on zn-8 staining, exposure to TDCIPP from 0.75–24 hpf resulted in a concentration dependent decrease in ocular area and pigmentation, and there was a systemic decrease in pigmentation across the entire embryo. In addition, zn 8 based immunostaining also revealed a deficiency of neuron formation within the eye. These phenotypes were consistent with known morphants of *otx1a*, *otx1b*, *smarca5* and *paics*, genes which regulate eye development.^{50, 51} Surprisingly, transcript levels of *otx1a*, *otx1b* and *paics* were increased in TDCIPP exposures. Therefore, abnormalities seen in eye development may have been driven by a decrease in transcript levels of *smarca5*, as decreased *smarca5* is known to lead to smaller eye morphology as well as deficiencies in neuronal numbers and organization.⁵⁰

Collectively, our data suggest that epiboly defects and dorsalization observed in TDCIPP-exposed embryos are primarily due to mesodermal disruption during somitogenesis. The progression of these phenotypes is likely independent of a direct impact on BMP signaling pathways even though TDCIPP-treated embryos phenocopied DMP-treated embryos at 24 hpf. These effects are stronger when exposures are initiated during cleavage and early blastula and may potentially be due to delayed activation of the zygotic genome – an effect that may alter the normal trajectory of embryonic development and lead to impacts on tissue differentiation and organogenesis. Future studies are needed to better understand the mechanisms underlying TDCIPP-induced epiboly defects as well as mechanisms linking epiboly defects and mesodermal disruption. As early developmental processes are conserved across all vertebrates, our findings suggest that TDCIPP has the potential to induce similar effects following *in utero* exposure in mammals.

Supplementary Material

Refer to Web version on PubMed Central for supplementary material.

Acknowledgements:

Fellowship support was provided by UCR's Graduate Division to V.C. and NRSA T32 Training Program [T32ES018827] to S.M.V. Research support was provided by a National Institutes of Health grant [R01ES027576] and the USDA National Institute of Food and Agriculture Hatch Project [1009609] to D.C.V.

References

1. Webster WS; Lipson AH; Sulik KK; Opitz JM; Reynolds JF, Interference with gastrulation during the third week of pregnancy as a cause of some facial abnormalities and CNS defects. *American Journal of Medical Genetics* 2005, 31(3), 505–512.
2. Boué A; Boué J; Gropp A, Cytogenetics of pregnancy wastage. *Adv Hum Genet* 1985, 14, 1–57. [PubMed: 3887861]
3. Babb SG; Marrs JA, E-cadherin regulates cell movements and tissue formation in early zebrafish embryos. *Developmental Dynamics* 2004, 230(2), 263–277. [PubMed: 15162505]
4. Lepage SE; Bruce AEE, Zebrafish epiboly: Mechanics and Mechanisms. *Int J Dev Biol* 2010, 54(8–9), 1213–1228. [PubMed: 20712002]
5. Kane DA; Hammerschmidt M; Mullins MC; Maischein HM; Brand M; van Eeden F; Furutani Seiki M; Granato M; Haffter P; Heisenberg CP, The zebrafish epiboly mutants. *Development* 1996, 123(1), 47–55. [PubMed: 9007228]
6. McCollum CW; Ducharme NA; Bondesson M; Gustafsson JA, Developmental toxicity screening in zebrafish. *Birth Defects Research Part C: Embryo Today: Reviews* 2011, 93(2), 67–114.
7. Marczylo EL; Jacobs MN; Gant TW, Environmentally induced epigenetic toxicity: potential public health concerns. *Critical Reviews in Toxicology* 2016, 46(8), 676–700. [PubMed: 27278298]
8. Lange L; Marks M; Liu J; Wittler L; Bauer H; Piehl S; Bläß G; Timmermann B; Herrmann BG, Patterning and gastrulation defects caused by the. *Biol Open* 2017, 6(6), 752–764. [PubMed: 28619992]
9. Hoffman K; Garantziotis S; Birnbaum LS; Stapleton HM, Monitoring Indoor Exposure to Organophosphate Flame Retardants: Hand Wipes and House Dust. *Environmental Health Perspectives* 2015, 123(2), 160–165. [PubMed: 25343780]
10. Stapleton HM; Klosterhaus S; Eagle S; Fuh J; Meeker JD; Blum A; Webster TF, Detection of organophosphate flame retardants in furniture foam and U.S. house dust. *Environ Sci Technol* 2009, 43(19), 7490–5. [PubMed: 19848166]
11. Bradman A; Castorina R; Gaspar F; Nishioka M; Colón M; Weathers W; Egeghy PP; Maddalena R; Williams J; Jenkins PL; McKone TE, Flame retardant exposures in California early childhood education environments. *Chemosphere* 2014, 116, 61–6. [PubMed: 24835158]
12. Butt CM; Congleton J; Hoffman K; Fang M; Stapleton HM, Metabolites of organophosphate flame retardants and 2 ethylhexyl tetrabromobenzoate in urine from paired mothers and toddlers. *Environmental science & technology* 2014, 48(17), 10432–10438. [PubMed: 25090580]
13. Castorina R; Butt C; Stapleton HM; Avery D; Harley KG; Holland N; Eskenazi B; Bradman A, Flame retardants and their metabolites in the homes and urine of pregnant women residing in California (the CHAMACOS cohort). *Chemosphere* 2017, 179, 159–166. [PubMed: 28365501]
14. Ding J; Xu Z; Huang W; Feng L; Yang F, Organophosphate ester flame retardants and plasticizers in human placenta in Eastern China. *Sci Total Environ* 2016, 554–555, 211–7.
15. Ospina M; Jayatilaka NK; Wong LY; Restrepo P; Calafat AM, Exposure to organophosphate flame retardant chemicals in the U.S. general population: Data from the 2013–2014 National Health and Nutrition Examination Survey. *Environ Int* 2018, 110, 32–41. [PubMed: 29102155]
16. Carignan CC; Mínguez Alarcón L; Williams PL; Meeker JD; Stapleton HM; Butt CM; Toth TL; Ford JB; Hauser R; Team ES, Paternal urinary concentrations of organophosphate flame retardant

metabolites, fertility measures, and pregnancy outcomes among couples undergoing in vitro fertilization. *Environ Int* 2018, 111, 232–238. [PubMed: 29241080]

17. Dasgupta S; Vliet SM; Kupsco A; Leet JK; Altomare D; Volz DC, Tris(1,3 dichloro 2 propyl) phosphate disrupts dorsoventral patterning in zebrafish embryos. *PeerJ* 2017, 5, e4156. [PubMed: 29259843]
18. Kupsco A; Dasgupta S; Nguyen C; Volz DC, Dynamic Alterations in DNA Methylation Precede Tris(1,3 dichloro 2 propyl)phosphate Induced Delays in Zebrafish Epiboly. *Environ Sci Technol Lett* 2017, 4(9), 367–373. [PubMed: 28993812]
19. Fu J; Han J; Zhou B; Gong Z; Santos EM; Huo X; Zheng W; Liu H; Yu H; Liu C, Toxicogenomic responses of zebrafish embryos/larvae to tris(1,3 dichloro 2 propyl) phosphate (TDCPP) reveal possible molecular mechanisms of developmental toxicity. *Environ Sci Technol* 2013, 47(18), 10574–82. [PubMed: 23919627]
20. McGee SP; Cooper EM; Stapleton HM; Volz DC, Early zebrafish embryogenesis is susceptible to developmental TDCPP exposure. *Environ Health Perspect* 2012, 120, (11), 1585. [PubMed: 23017583]
21. Vliet SM; Ho TC; Volz DC, Behavioral screening of the LOPAC1280 library in zebrafish embryos. *Toxicol Appl Pharmacol* 2017, 329, 241–248. [PubMed: 28623180]
22. Kimmel CB; Ballard WW; Kimmel SR; Ullmann B; Schilling TF, Stages of embryonic development of the zebrafish. *Dev Dyn* 1995, 203(3), 253–310. [PubMed: 8589427]
23. Volz DC; Leet JK; Chen A; Stapleton HM; Katiyar N; Kaundal R; Yu Y; Wang Y, Tris(1,3 dichloro 2 propyl)phosphate Induces Genome Wide Hypomethylation within Early Zebrafish Embryos. *Environ Sci Technol* 2016, 50(18), 10255–63. [PubMed: 27574916]
24. Mitchell CA; Dasgupta S; Zhang S; Stapleton HM; Volz DC, Disruption of Nuclear Receptor Signaling Alters Triphenyl Phosphate Induced Cardiotoxicity in Zebrafish Embryos. *Toxicol Sci* 2018, 163(1), 307–318. [PubMed: 29529285]
25. Harvey SA; Sealy I; Kettleborough R; Fenyes F; White R; Stemple D; Smith JC, Identification of the zebrafish maternal and paternal transcriptomes. *Development* 2013, 140(13), 2703–10. [PubMed: 23720042]
26. Yozzo KL; Isales GM; Raftery TD; Volz DC, High content screening assay for identification of chemicals impacting cardiovascular function in zebrafish embryos. *Environ Sci Technol* 2013, 47(19), 11302–10. [PubMed: 24015875]
27. Leet JK; Lindberg CD; Bassett LA; Isales GM; Yozzo KL; Raftery TD; Volz DC, High content screening in zebrafish embryos identifies butafenacil as a potent inducer of anemia. *PLoS One* 2014, 9(8), e104190. [PubMed: 25090246]
28. Lee MT; Bonneau AR; Giraldez AJ, Zygotic genome activation during the maternal to zygotic transition. *Annu Rev Cell Dev Biol* 2014, 30, 581–613. [PubMed: 25150012]
29. Lee MT; Bonneau AR; Takacs CM; Bazzini AA; DiVito KR; Fleming ES; Giraldez AJ, Nanog, Pou5f1 and SoxB1 activate zygotic gene expression during the maternal to zygotic transition. *Nature* 2013, 503(7476), 360–4. [PubMed: 24056933]
30. Du S; Draper BW; Mione M; Moens CB; Bruce A, Differential regulation of epiboly initiation and progression by zebrafish Eomesodermin A. *Dev Biol* 2012, 362(1), 11–23. [PubMed: 22142964]
31. Pei W; Noushmehr H; Costa J; Ouspenskaia MV; Elkahlon AG; Feldman B, An early requirement for maternal FoxH1 during zebrafish gastrulation. *Dev Biol* 2007, 310(1), 10–22. [PubMed: 17719025]
32. Wang Y; Zhou L; Li Z; Li W; Gui J, Apolipoprotein C1 regulates epiboly during gastrulation in zebrafish. *Sci China Life Sci* 2013, 56(11), 975–84. [PubMed: 24203452]
33. Tucker JA; Mintzer KA; Mullins MC, The BMP signaling gradient patterns dorsoventral tissues in a temporally progressive manner along the anteroposterior axis. *Dev Cell* 2008, 14(1), 108–19. [PubMed: 18194657]
34. Yabe T; Takada S, Mesogenin causes embryonic mesoderm progenitors to differentiate during development of zebrafish tail somites. *Dev Biol* 2012, 370(2), 213–22. [PubMed: 22890044]
35. Bouldin CM; Manning AJ; Peng YH; Farr GH, 3rd; Hung KL; Dong A; Kimelman D, Wnt signaling and tbx16 form a bistable switch to commit bipotential progenitors to mesoderm. *Development* 2015, 142(14), 2499–507. [PubMed: 26062939]

36. Garnett AT; Han TM; Gilchrist MJ; Smith JC; Eisen MB; Wardle FC; Amacher SL, Identification of direct T box target genes in the developing zebrafish mesoderm. *Development* 2009, 136(5), 749–60. [PubMed: 19158186]
37. Manning AJ; Kimelman D, Tbx16 and Msn1 are required to establish directional cell migration of zebrafish mesodermal progenitors. *Dev Biol* 2015, 406(2), 172–85. [PubMed: 26368502]
38. Mueller RL; Huang C; Ho RK, Spatio temporal regulation of Wnt and retinoic acid signaling by tbx16/spadetail during zebrafish mesoderm differentiation. *BMC Genomics* 2010, 11, 492. [PubMed: 20828405]
39. Pyati UJ; Webb AE; Kimelman D, Transgenic zebrafish reveal stage specific roles for Bmp signaling in ventral and posterior mesoderm development. *Development* 2005, 132(10), 2333–43. [PubMed: 15829520]
40. Schier AF; Talbot WS, Molecular genetics of axis formation in zebrafish. *Annu Rev Genet* 2005, 39, 561–613. [PubMed: 16285872]
41. Fior R; Maxwell AA; Ma TP; Vezzano A; Moens CB; Amacher SL; Lewis J; Saude L, The differentiation and movement of presomitic mesoderm progenitor cells are controlled by Mesogenin 1. *Development* 2012, 139(24), 4656–65. [PubMed: 23172917]
42. Oates AC; Rohde LA; Ho RK, Generation of segment polarity in the paraxial mesoderm of the zebrafish through a T box dependent inductive event. *Dev Biol* 2005, 283(1), 204–14. [PubMed: 15921674]
43. Yu PB; Hong CC; Sachidanandan C; Babitt JL; Deng DY; Hoyng SA; Lin HY; Bloch KD; Peterson RT, Dorsomorphin inhibits BMP signals required for embryogenesis and iron metabolism. *Nat Chem Biol* 2008, 4(1), 33–41. [PubMed: 18026094]
44. Rohde LA; Oates AC; Ho RK, A crucial interaction between embryonic red blood cell progenitors and paraxial mesoderm revealed in spadetail embryos. *Dev Cell* 2004, 7(2), 251–62. [PubMed: 15296721]
45. Leet JK; Hipszler RA; Volz DC, Butafenacil: A positive control for identifying anemia and variegate porphyria inducing chemicals. *Toxicol Rep* 2015, 2, 976–983. [PubMed: 28962437]
46. Jacob E; Drexel M; Schwerte T; Pelster B, Influence of hypoxia and of hypoxemia on the development of cardiac activity in zebrafish larvae. *Am J Physiol Regul Integr Comp Physiol* 2002, 283(4), R911–7. [PubMed: 12228061]
47. Miura GI; Yelon D, A guide to analysis of cardiac phenotypes in the zebrafish embryo. *Methods Cell Biol* 2011, 101, 161–80. [PubMed: 21550443]
48. Seeley M; Huang W; Chen Z; Wolff WO; Lin X; Xu X, Depletion of zebrafish titin reduces cardiac contractility by disrupting the assembly of Z discs and A bands. *Circ Res* 2007, 100(2), 238–45. [PubMed: 17170364]
49. Will RD; Eden M; Just S; Hansen A; Eder A; Frank D; Kuhn C; Seeger TS; Oehl U; Wiemann S, Myomasp/LRRC39, a Heart and Muscle Specific Protein, Is a Novel Component of the Sarcomeric M Band and Is Involved in Stretch Sensing Novelty and Significance. *Circulation research* 2010, 107(10), 1253–1264. [PubMed: 20847312]
50. Gross JM; Perkins BD; Amsterdam A; Egana A; Darland T; Matsui JI; Sciascia S; Hopkins N; Dowling JE, Identification of zebrafish insertional mutants with defects in visual system development and function. *Genetics* 2005, 170(1), 245–61. [PubMed: 15716491]
51. Lane BM; Lister JA, Otx but not Mitf transcription factors are required for zebrafish retinal pigment epithelium development. *PLoS One* 2012, 7(11), e49357. [PubMed: 23139843]

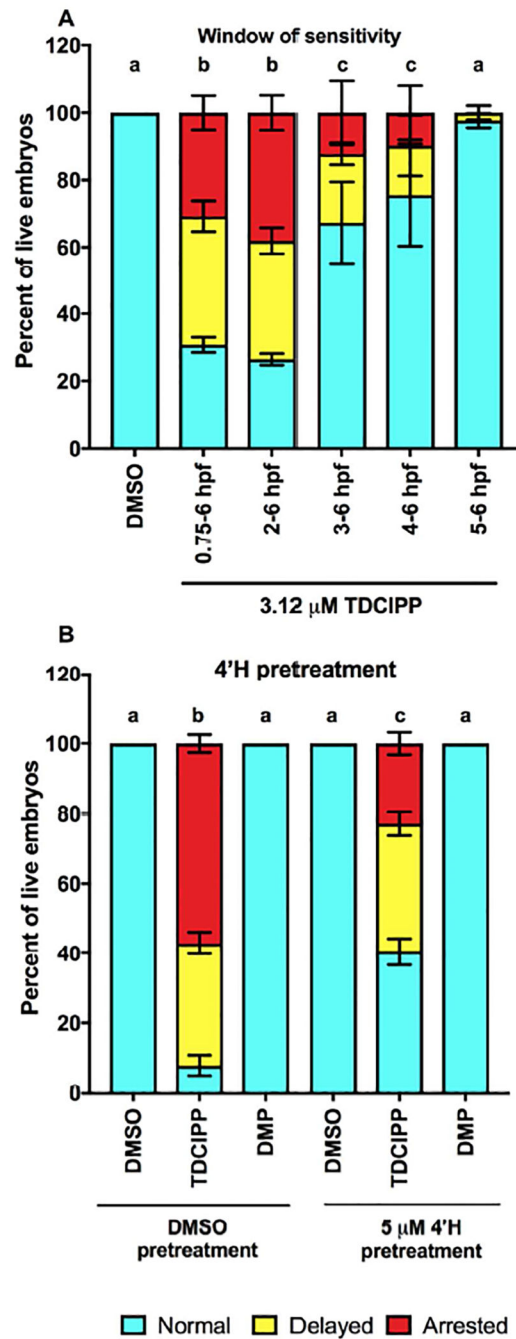


Figure 1.

Sensitive window of exposure and effects of 4'H pre-treatment on TDCIPP-induced epiboly defects at 6 hpf. 2–3 hpf represents the most sensitive window for TDCIPP-induced effects on epiboly at 6 hpf (A). 4'H pre-treatment partially blocks TDCIPP-induced epiboly defects at 6 hpf (B). 100% of embryos were normal across all DMSO control replicates. Bars with dissimilar letters are significantly different ($p < 0.05$).

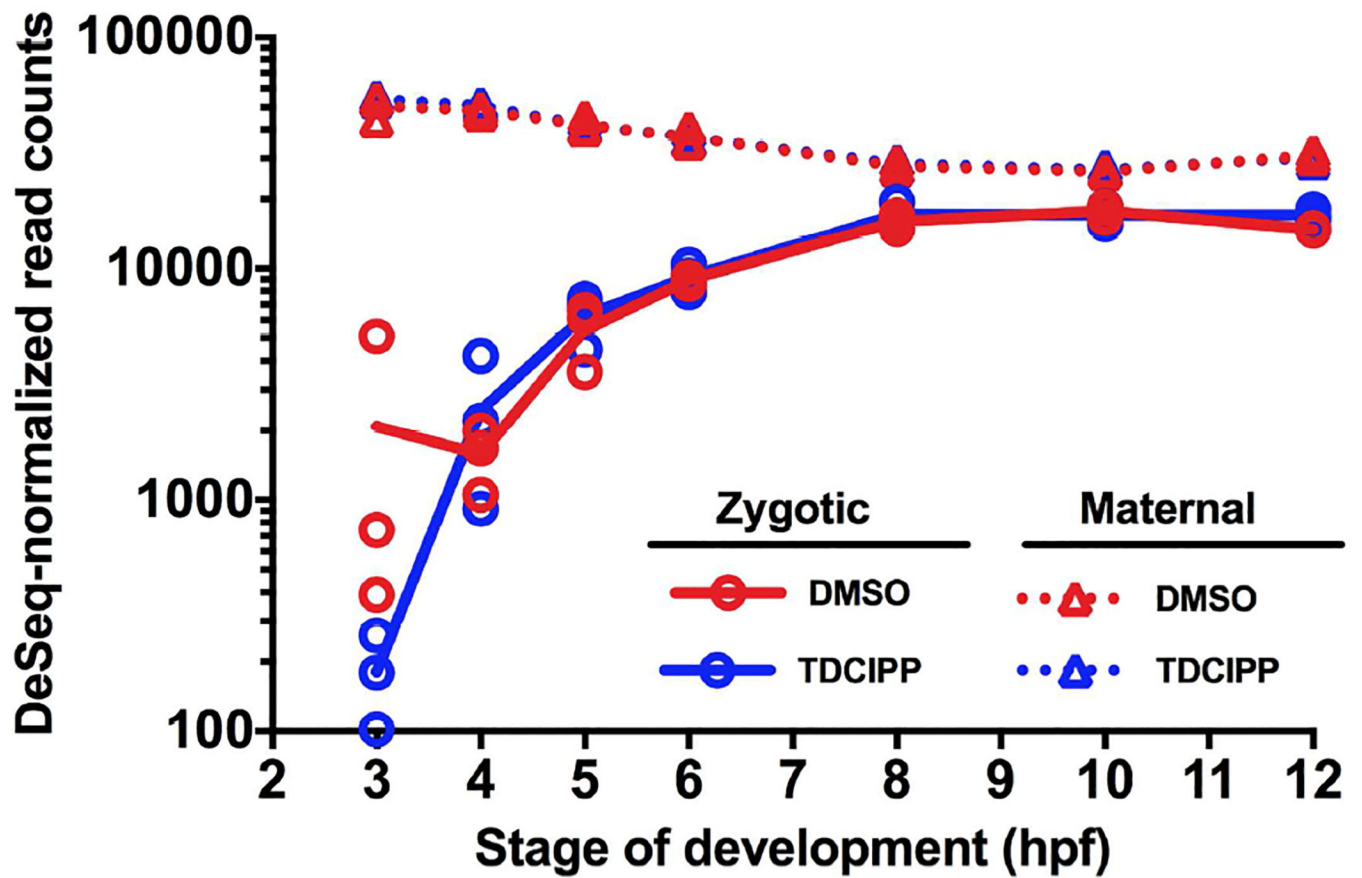


Figure 2. Effect of TDCIPP on activation of the zygotic genome. Based on normalized read counts, TDCIPP exposures induce a slight (albeit non significant) ~1-hr delay in activation of zygotic genome at 3 hpf.

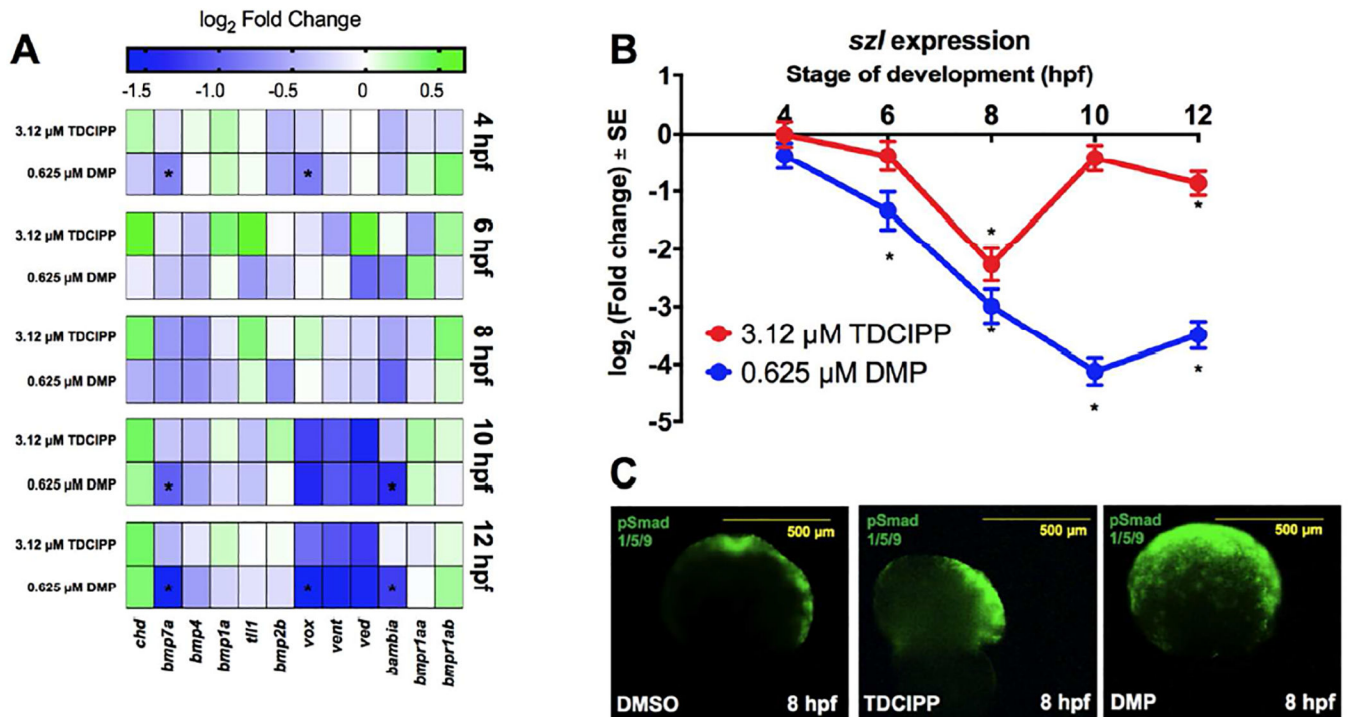


Figure 3.

Impact of TDCIPP on BMP signaling. While exposure to 0.625 μM DMP decreased BMP specific transcripts between 4 and 12 hpf, these transcripts are not affected by exposure to 3.12 μM TDCIPP (A). The only exception was *sizzled (szl)*, where mRNA levels were strongly decreased in both treatments (B). Immunostaining with anti phospho SMAD 1/5/9 also showed minimal effects of TDCIPP on BMP gradients (C); DMSO- and TDCIPP-treated embryos showed a normal BMP gradient from ventral to dorsal side at 8 hpf, whereas DMP treated embryos showed a disrupted gradient. Asterisk denotes significant difference relative to time matched vehicle controls ($p_{adj} < 0.05$).

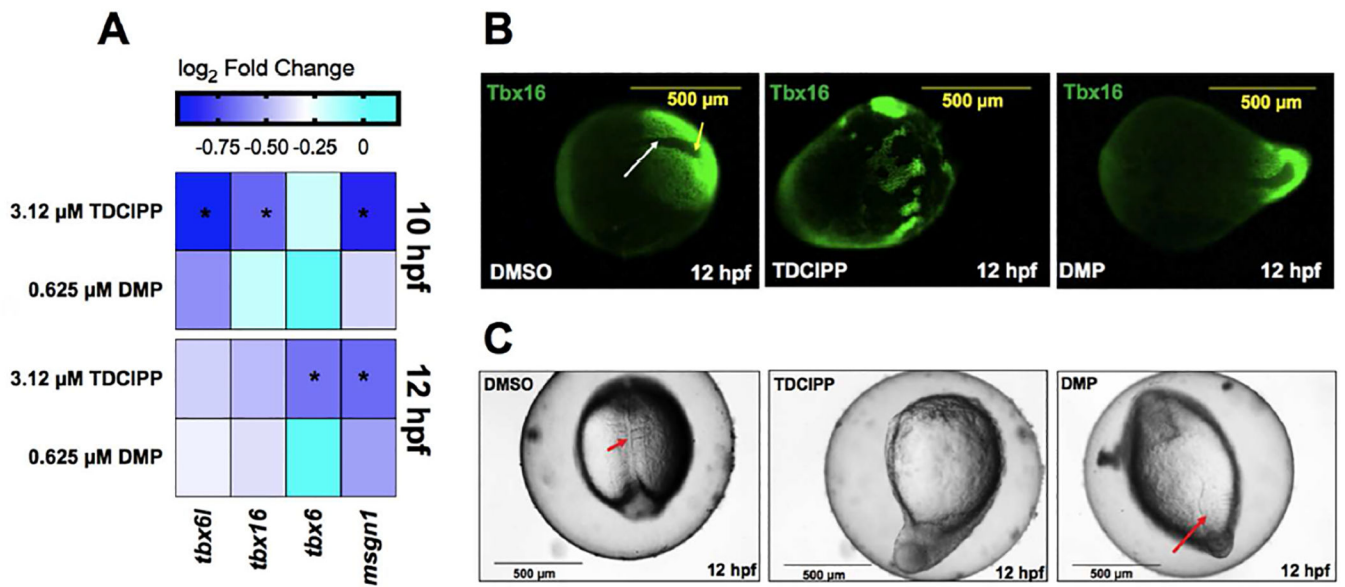


Figure 4.

TDCIPP-induced effects on mesoderm development and differentiation. mRNA levels of mesoderm regulating genes (*tbx6*, *tbx16*, *tbx6l* and *msgn1*) were decreased in 3.12 μM TDCIPP treatments between 10 and 12 hpf (beginning of somitogenesis), whereas DMP did not affect these transcripts (A). Immunostaining with anti-VegT (*tbx16*) antibody at 12 hpf revealed normal patterning of paraxial mesodermal tissues and localization towards the tail bud at 12 hpf in DMSO- and DMP-treated embryos, but disrupted localization in 3.12 μM TDCIPP-treated embryos (B). Yellow arrow points to tail bud and white arrow points to notochord. Higher magnification of the embryonic structure revealed that, while TDCIPP-treated embryos at 12 hpf lacked a well-developed notochord and somites were absent, DMP-treated embryos possessed somites in the tail that are broader and more radially extended than somites within vehicle controls (red arrow) (C). Asterisk denotes significant difference relative to time matched vehicle controls ($p_{adj} < 0.05$).

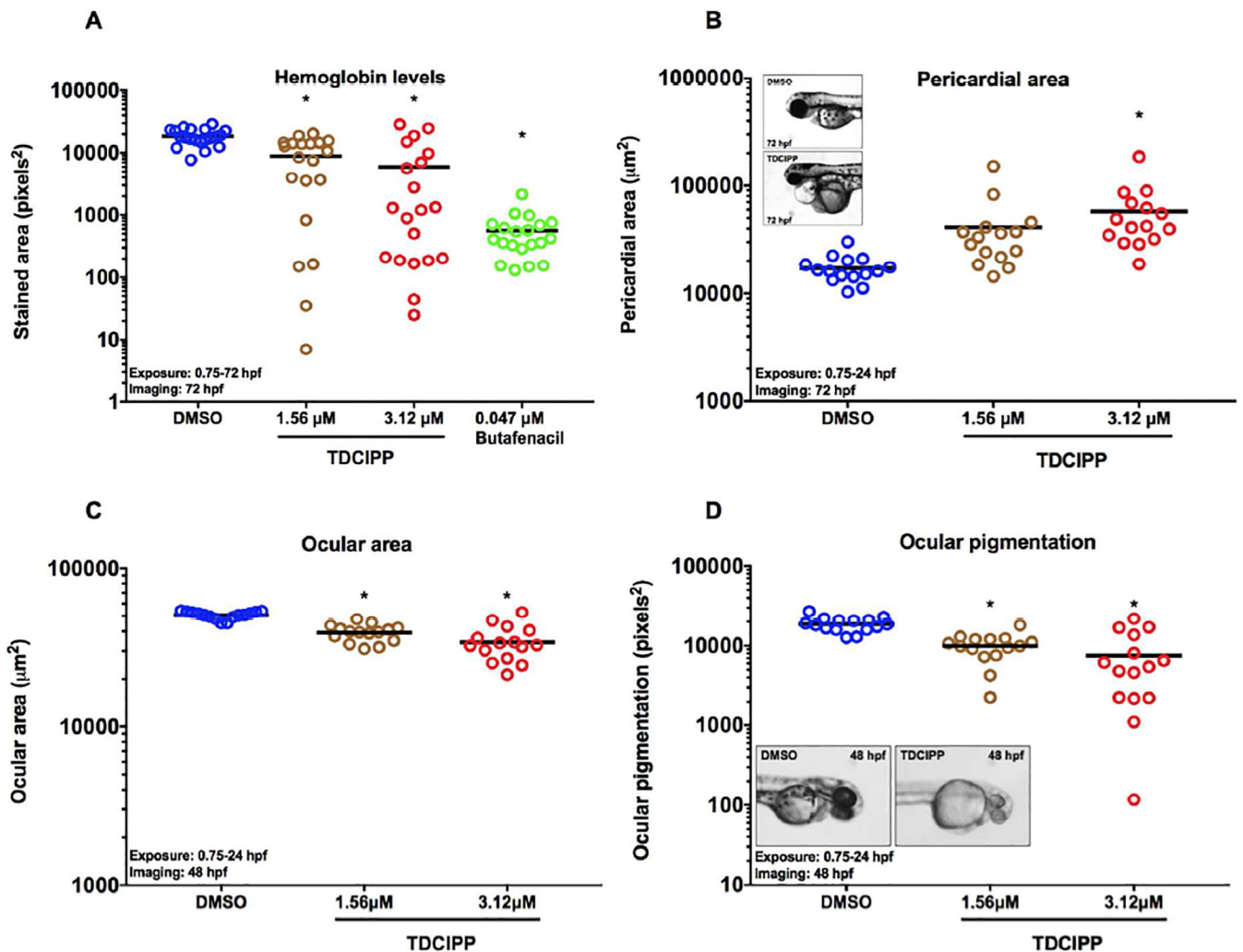


Figure 5.

TDCIPP-induced effects on hemoglobin levels as well as cardiac and ocular development. TDCIPP-treatments induce a concentration-dependent decrease in hemoglobin levels at 72 hpf when treatments are initiated at 0.75 hpf (N=20 embryos per treatment). Butafenacil was used as a positive control for chemically induced anemia (A). TDCIPP exposure from 0.75–24 hpf results in a concentration dependent increase in pericardial area at 72 hpf (B) and concentration dependent decrease in ocular area (C) and ocular pigmentation (D) at 48 hpf. N=15 embryos per treatment in each case. Insets show occurrence of tube hearts (B) and lack of pigmentation (D) in representative embryos treated with 3.12 mM TDCIPP. In all cases, asterisk denotes significant difference relative to vehicle controls ($p < 0.05$), and black line denotes the treatment mean.